Volume 11
Number 47
21 December 2020
Pages 12593–12878

Chemical Science

10TH ANNIVERSARY

rsc.li/chemical-science

ISSN 2041-6539

ROYAL SOCIETY OF CHEMISTRY

EDGE ARTICLE

Han Sun, Christian P. R. Hackenberger *et al.*

Combining free energy calculations with tailored enzyme activity assays to elucidate substrate binding of a phospho-lysine phosphatase

Chemical Science

ROYAL SOCIETY OF CHEMISTRY

EDGE ARTICLE

View Article Online
View Journal | View Issue

Cite this: *Chem. Sci.*, 2020, **11**, 12655

All publication charges for this article have been paid for by the Royal Society of Chemistry

Combining free energy calculations with tailored enzyme activity assays to elucidate substrate binding of a phospho-lysine phosphatase†

Anett Hauser,[ab] Songhwan Hwang,[c] Han Sun *[c] and Christian P. R. Hackenberger *[ab]

Received 19th July 2020
Accepted 7th September 2020

DOI: 10.1039/d0sc03930f

rsc.li/chemical-science

Studying enzymes that are involved in the regulation of dynamic post-translational modifications (PTMs) is of key importance in proteomics research. Such investigations can be particularly challenging when the modification itself is intrinsically labile. In this article, we elucidate the enzymatic activity of *Phospholysine Phosphohistidine Inorganic Pyrophosphate Phosphatase* (LHPP) towards different *O*- and *N*-phosphorylated peptides by a combined experimental and computational approach. LHPP has been previously described to hydrolyze the phosphoramidate bonds in different small molecule substrates, including phosphorylated lysine (pLys). Taking the instability of the phosphoramidate bond into account, we conducted a carefully adjusted enzymatic assay with various pLys pentapeptides to confirm enzymatic phosphatase activity with LHPP. Molecular docking was employed to explore possible binding poses of the substrates in complex with the enzyme. Molecular dynamics based free energy calculations, which are unique in their accuracy and solid theoretical basis, were further applied to predict relative binding affinity of different substrates. Comparison of simulations with experiments clearly suggested a distinct binding motif of pLys peptides as well as a very narrow promiscuity of LHPP. We believe this integrated approach can be widely adopted to study the structure and interaction of poorly characterized enzyme–substrate complexes, in particular with synthetically challenging or labile substrates.

Introduction

A balanced interplay of protein phosphorylation and dephosphorylation is a key factor to functioning cellular processes.[1–3] So far, many detailed studies on structure–activity relationships, substrates and mechanisms have been conducted to understand the various processes taking place during the introduction of phosphate groups into proteins by kinases.[4–6] Meanwhile, enzymes responsible for the cleavage of phosphates or other phosphate ester derivatives like phosphoramidates or phosphorothioates are less often subjects of studies.[7] Challenging aspects include short-term interactions with substrates, high complexity regarding evolutionary development, regulatory pathways and possible substrates as well as experimental demands, especially if the phosphorylated peptide substrates have a low stability profile.[7]

A prime example in this regard is the *Phospholysine Phosphohistidine Inorganic Pyrophosphate Phosphatase* (LHPP). First reported in 1997 by Hiraishi *et al.*, LHPP was isolated from bovine liver. Subsequently the enzymatic hydrolase activity was shown, first for pyrophosphate (PP_i) and imidodiphosphate (PNP), later for the single amino acids ε-phospho-lysine (pLys) and 3-phospho-histidine (3-pHis).[8,9] While researchers could observe slightly higher activity for PNP compared to PP_i (0.44 μmol min^{-1} mg^{-1} and 0.11 μmol min^{-1} mg^{-1} released phosphate at pH 8.2 in the presence of 1 mM $MgCl_2$) as well as for pLys compared to pHis (1.22 μmol min^{-1} mg^{-1} and 1.09 μmol min^{-1} mg^{-1} released phosphate at pH 8.2 in the presence of 1 mM $MgCl_2$), no structural information about the binding event of pLys or pHis residues to LHPP is currently known. Furthermore, besides small molecules, no endogenous pLys-containing peptide or protein substrates for LHPP were reported to date and thus, no standardized value that describes catalytic potency has been established. Nevertheless, LHPP is known to occur in several species[10] and to have an influence in different diseases.[11–13] Very recently, its role as a tumor suppressor was highlighted by Hindupur *et al.*, Zheng *et al.* and Li *et al.* shortly afterwards.[12–14] In all cases, findings were supported by knockout/overexpression experiments, but no specific substrate was investigated. Moreover, LHPP is assigned to the haloacid dehydrogenase (HAD) super-family of hydrolases,[15] but

[a]*Department of Chemical Biology II, Leibniz-Forschungsinstitut für Molekulare Pharmakologie (FMP), Berlin, Germany. E-mail: hackenbe@fmp-berlin.de*

[b]*Institute for Chemistry, Humboldt-Universität zu Berlin, Berlin, Germany*

[c]*Group of Structural Chemistry and Computational Biophysics, Leibniz-Forschungsinstitut für Molekulare Pharmakologie (FMP), Berlin, Germany. E-mail: hsun@fmp-berlin.de*

† Electronic supplementary information (ESI) available. See DOI: 10.1039/d0sc03930f

its catalytic mechanism remains unknown and therefore, information about the scope or sequence dependency is missing.[16] Although the enzymatic activity was shown to be higher for pLys, all the later findings described LHPP in the role of a phosphoramidate hydrolase selective for pHis.[17,18]

Although the phosphorylation of lysine residues was described for the first time more than 45 years ago, its biological role has been, to date, only rudimentarily elucidated. Initially described to occur as an acid-labile group in histone H1,[19,20] pLys could be detected in rat liver *in vivo* later.[21,22] The reported chemical and thermal instability[23] has hampered further identification and characterization with conventional proteomics techniques. Despite recent reports on incident pLys detection by empirico-statistical methods,[24,25] an in-depth study on endogenous pLys sites has yet to be published. Along those lines, also no enzyme being selectively active on phosphorylated lysine peptides or proteins is known so far. It should be noted that the phosphoramidate bond in pLys is intrinsically labile at physiological pH, which means that high background hydrolysis during enzymatic studies is to be expected.[23] Our group has recently developed suitable synthetic and analytical methods to advance research questions for this most intriguing post-translational modification.[23,26–29] Here, we present a systematic study to elucidate the structure–activity relationship as well as the interaction of different *N*- and *O*-phosphorylated substrates with LHPP including phosphorylated lysine. In particular, we probed the enzymatic activity of LHPP towards phosphate- or phosphoramidate-containing peptide substrates with different steric and electronical demand. All peptidic substrates were obtained *via* elaborated organic synthetic protocols specifically optimized for each compound class. This was particularly important for studying the hydrolase activity of pLys-containing peptides due to their intrinsic lability. It has been shown that the phosphorous–nitrogen bond was hydrolyzed very fast under acidic conditions and at elevated temperatures.[23] For example, the half-life time of pLys is approx. 2.5 h at room temperature and pH 3.5 or below and even less than 1 h at 60 °C and neutral pH.[23] Therefore, a fine-tuned assay with less delay between each step was required.

Since no structural information about the binding mode of phosphoramidate substrates was available, we used molecular docking originating from a known crystal structure with a bound pyrophosphate substrate to explore possible binding poses. To further evaluate binding of different substrates quantitatively, we used molecular dynamics (MD) based alchemical free energy calculations, which has emerged in recent years as a promising tool for *in silico* drug optimizations,[30,31] quantifying protein–protein interactions[32] and understanding drug resistance.[33] Taking advantage of high accuracy of this first-principle statistical mechanics-based method, we predicted free energy changes ($\Delta\Delta G$) upon mutation in the pLys-peptides for a number of different docking poses. Comparison of the predicted free energy changes with the experimental rates verified enzymatic activity for pLys dephosphorylation and pointed to low substrate promiscuity.

Results and discussion

Phosphoramidate hydrolase and phosphatase assay to evaluate the LHPP substrate scope

To minimize phosphoramidate bond hydrolysis even without enzyme being present, fast sample preparation, distinct pH adjustment and storage at low temperature were crucial. Whereas previous studies to monitor LHPP activity relied on detection of released inorganic phosphate (P_i) using Rosenberg's reagent[9] or malachite green,[8,10] we considered both methods as too time consuming to meet the stability profile of pLys peptides. State of the art real-time detection of released P_i can be conducted conveniently in cuvette- or microplate-based experiments and we desired a similar set up to conduct kinetic experiments. The EnzChek® Phosphate Assay kit enables continuous measurement of released P_i by the phosphate dependent conversion of 2-amino-6-mercapto-7-methylpurine riboside to a UV-active thione.[34] In order to identify optimal assay conditions, we first conducted LHPP activity measurements with the previously reported substrate pLys (**1a**).[9,23] Varying the concentration of **1a** and LHPP at pH 7.4, we identified 100 μM substrate **1a** in a 200 μL reaction volume with 0.25 μg enzyme (7.4×10^{-3} nmol, 0.037 μM, 3.7×10^{-4} eq.) as suitable for conducting enzyme kinetics within 90 minutes incubation time. It should be noted that pLys background hydrolysis gave a significant absorbance already at the starting point of each experiment (Fig. S1†). Any possible synthesis route of phospho-lysine or pLys-peptides would fail to deliver pure phosphorylated substrates, since either the conversion would not be quantitative or the phosphoramidate would partially hydrolyze during purification.[23,28,35] Hence, we conducted the kinetic measurements with mixtures of pLys and Lys + P_i.

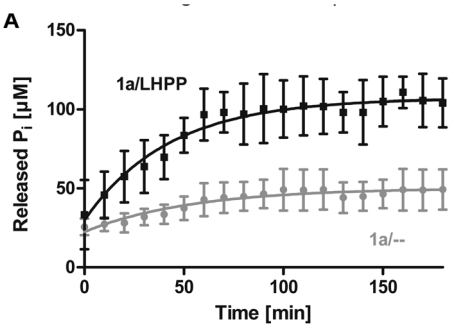

B

substrate	Without LHPP			
	v_0 [M·s^{-1}]	Error ±	k [s^{-1}]	Error ±
1a	$2.10 \cdot 10^{-9}$	$3.65 \cdot 10^{-10}$	$3.47 \cdot 10^{-5}$	$4.13 \cdot 10^{-6}$
	With LHPP			
	v_0 [M·s^{-1}]	Error ±	k [s^{-1}]	Error ±
	$2.00 \cdot 10^{-8}$	$4.43 \cdot 10^{-10}$	$2.25 \cdot 10^{-4}$	$1.86 \cdot 10^{-5}$

Fig. 1 (A) Example for kinetics of 100 μM **1a** with 0.25 μg LHPP over 180 min. Amount of released inorganic phosphate without (—) or with (—) LHPP being present. (B) Initial rates and first order rate constants of the kinetic studies of **1a**.

Additionally, the intrinsic lability led to more P_i release over time even without enzyme being present (Fig. 1A, grey line). Therefore, we used the difference between the detected value for released phosphate from incubation with LHPP (Fig. 1A, black line) and the value without addition of enzyme (Fig. 1A, grey line) to evaluate the enzymatic hydrolysis. As shown for 100 μM **1a**, more than 40% of substrate were hydrolyzed after the experiment without LHPP being present. This means, roughly 50 μM pLys were degraded by LHPP, according to 50% enzymatically hydrolyzed substrate, after 60 minutes, when the conversion was complete. With the standardized conditions, we were able to determine kinetic parameters, *e.g.* initial rates v_0 and first order rate constant k, from the measured data. Fig. 1B shows the data for the sample experiment of 100 μM pLys **1a** without enzyme and with 0.25 μg LHPP. It can be seen that the hydrolysis occurred one magnitude faster upon LHPP addition and thus, the enzyme could accelerate the reaction rate despite the substrate's intrinsic lability.

Next, we investigated the enzymatic activity of LHPP towards different types of phosphorylated amino acids (Fig. 2A), which were synthesized following published protocols.[36,37] LHPP activity with various substrates was determined on a microplate reader by photometric detection of released inorganic phosphate (ESI, Section 1†). All substrates were incubated at a concentration of 100 μM in 200 μL of 50 mM Tris–HCl buffer containing 1 mM $MgCl_2$ at pH 7.8 in the presence or absence of 0.25 μg LHPP (3.7×10^{-4} eq., 7.4×10^{-3} nmol, 0.037 μM). Absorbance was measured every ten minutes for 90 min. In accordance with the results published by Hiraishi *et al.* (see above),[9] phosphorylated lysine monomer **1a** was hydrolyzed at a rate of 0.88 μmol $min^{-1} \cdot mg^{-1}$, which corresponded to 56.26% enzymatically hydrolyzed pLys after 90 min (background hydrolysis subtracted). For the other *N*-phospho-amino acids (pHis **1f**, pArg **1e**) and for the phosphates (pSer **1b**, pThr **1c**, pTyr **1d**) drastically lower values for the hydrolyzed substrates were observed after 90 min (17.57%, 6.64%, 5.75%, 3.67%, 4.81%, respectively, see Fig. 3A).

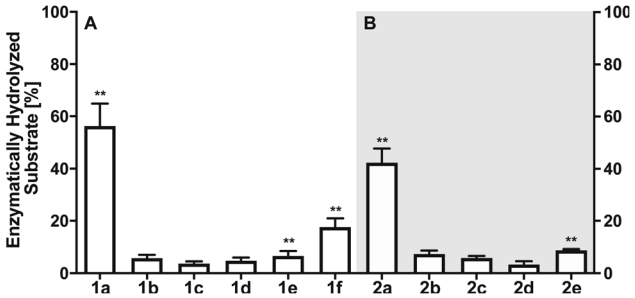

Fig. 3 (A) Percentage of enzymatically hydrolyzed substrate after 90 minutes of incubation of monomeric phospho-amino acids **1a–1f** with LHPP. (B) Percentage of enzymatically hydrolyzed substrate after 90 minutes of incubation of differently phosphorylated pentapeptides **2a–2e** with LHPP. Experiments have been conducted as biological and technical triplicates. ** percentage of hydrolyzed substrate without enzyme being present has been subtracted.

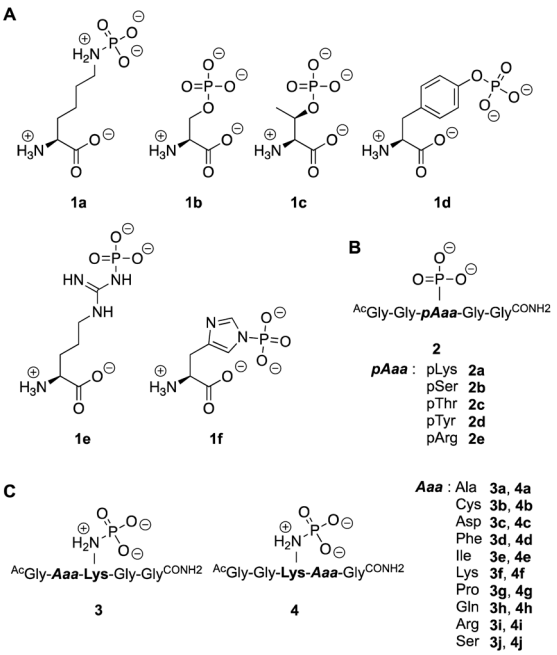

Fig. 2 Substrates employed in this study. Different phospho-amino acids (A) and phospho-peptides (B) to examine the activity towards phosphates and phosphoramidates. (C) Pentapeptides to study the neighboring effect of amino acid side chains.

To evaluate different *N*- and *O*-phosphorylated peptide substrates of LHPP we synthesized a set of simple pentapeptides with the sequence ^{Ac}GlyGly*pAaa*GlyGly^{CONH_2} (*pAaa*: pLys **2a**, pSer **2b**, pThr **2c**, pTyr **2d** or pArg **2e**) (Fig. 2B). Even though we intended to analyze the pHis substrate as well, the reaction to form the corresponding pHis peptide could neither be driven to sufficient conversion nor be purified from the phosphorylation reagent or the unphosphorylated peptide and was thus excluded from this study. For the synthesis of pLys peptides, we used our previously reported protocols to obtain pLys peptides.[23] This allowed us to take advantage of the chemoselectivity during a reaction between an azide and a phosphite for the incorporation of a photocaged pLys precursor at a given site in the peptide starting from commercially available Fmoc-protected azido-lysine. Subsequently, the Staudinger-phosphite reaction with tris(1-(2-nitrophenyl)ethyl) phosphite and subsequent photodeprotection yielded desired, free pLys (ESI, Section 2.1†).

The enzymatic activity observed for the pentapeptides corroborated with the amino acid findings from before, for instance 37.90% enzymatically hydrolyzed ^{Ac}GlyGlypLysGlyGly^{CONH_2} **2a** after 90 min, while all other substrates showed significantly lower hydrolysis yield (**2b:** 7.37%, **2c:** 5.86%, **2d:** 3.34%, **2e:** 8.78%, Fig. 3B). To our knowledge, this is the first time that *N*- and *O*-phosphorylated peptides have been assayed with LHPP, which serves as corroboration that LHPP is a rather a selective phosphoramidate hydrolase but not a phosphate ester hydrolase. In addition, the decreased hydrolysis yield obtained for peptide **2a** when compared to **1a** points towards a narrower substrate scope.

To investigate this further, we systematically evaluated two additional sets of peptides, in which the amino acids N- or C-

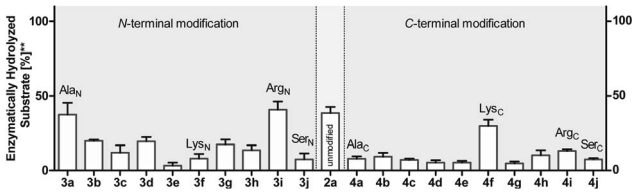

Fig. 4 Phosphoramidate hydrolysis yields for N- and C-terminally modified pentapeptides after 90 min of incubation. Experiments have been conducted as biological and technical triplicates. ** percentage of hydrolyzed substrate without enzyme being present has been subtracted.

terminal to the pLys residue were exchanged (^{Ac}Gly*Aaa*pLysGlyGly^{CONH_2} **3**, ^{Ac}GlyGlypLys*Aaa*Gly^{CONH_2} **4**, *Aaa*: Ala, Cys, Asp, Phe, Ile, Lys, Pro, Gln, Arg, Ser, Fig. 2C). The amino acid substitutions were chosen to address different electronic and steric scenarios. All substrates were assayed as described above. Indeed, we observed a distinct impact on the phosphoramidates hydrolase activity of LHPP by modifications adjacent to the phosphorylation site (Fig. 4). While most of the modifications led to a drastic decrease of enzymatic hydrolysis, only peptides **3a** and **3i** with N-terminal Ala and Arg or peptide **4f** with C-terminal Lys could retain or surpass the hydrolysis yields after 90 minutes (**3a**: 37.33%, **3i**: 40.70%, **4f**: 29.81%, respectively) (Fig. 4). These findings were particularly interesting since modifications with switched positions (C-terminal Ala **4a** and Arg **4j** or N-terminal Lys **3f**) displayed reduced conversions. Interestingly, peptides **3c** and **4c** containing a negatively charged Asp residue showed hydrolysis values as compared to substrates with positively charged residues (Lys: **3f** and **4f**, Arg: **3i** and **4i**), in which only up to one third of P_i could be released. These observations hint towards electrostatic repulsion of **3c** and **4c** in the binding pocket of LHPP as it exhibits a high negative electron density as discussed later, thus further suggesting that LHPP is sensitive to sequence alterations and accepts only a limited scope of pLys substrates. Similar findings have been reported recently for LHPP activity on histidine phosphorylations by Choi *et al.* as mentioned above.[18]

Next, we evaluated the kinetics for the hydrolysis of pLys peptides with and without LHPP addition for peptides **2a**, **3a** and **3j**, which included the substrates with the highest and lowest hydrolysis yields after 90 min (Fig. 5 and Table 1). We observed the highest first order rate constants with LHPP for

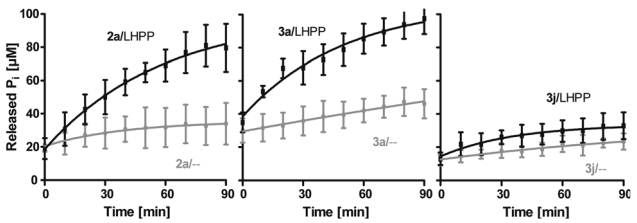

Fig. 5 Kinetics for **2a**, **3a** and **3j**. The rate of background hydrolysis was strongly impacted by the peptide sequence. — with LHPP, — without addition of LHPP.

Table 1 Initial rates and first order rate constants of the kinetic studies of **2a**, **3a** and **3i**

Substrate	v_0 [M s^{-1}]	Error ±	k [s^{-1}]	Error ±
Without LHPP				
2a	4.95×10^{-9}	2.16×10^{-9}	3.59×10^{-5}	4.35×10^{-6}
3a	2.48×10^{-9}	1.53×10^{-10}	5.60×10^{-5}	2.95×10^{-6}
3j	3.09×10^{-9}	2.58×10^{-10}	2.47×10^{-5}	2.00×10^{-6}
With LHPP				
2a	1.97×10^{-8}	5.80×10^{-11}	3.44×10^{-4}	2.07×10^{-5}
3a	2.72×10^{-8}	2.26×10^{-9}	4.29×10^{-4}	3.93×10^{-5}
3j	6.46×10^{-9}	1.94×10^{-9}	4.24×10^{-5}	4.90×10^{-6}

peptide **3a**, which was one order of magnitude higher than for **3j**. In addition, the experiments conducted without LHPP pointed towards a distinct intrinsic lability for each substrate depending on the amino acid sequence and revealed a higher lability for peptide **3a** as compared to the other peptides. As already observed with pLys **1a**, the background hydrolysis could have a significant impact on the obtained amount of enzymatically hydrolyzed substrate. This could be observed with **2a** but was particularly clear in the case of Ala-modified substrate **3a**, which yielded more than 40% hydrolysis without LHPP being present and thus, only approx. 38% enzymatically hydrolyzed substrate was eventually observed.

Also, both, the higher initial rate v_0 and the increased first order rate constant k indicated higher substrate lability in reactions without enzyme being present (Table 1, upper part). We hypothesize that the increased stability of Ser-modified peptide **3j** could be based on hydrogen bonds formed between the protons on ε-nitrogen in pLys and the free electron pairs on the Ser oxygen, which resulted in a decreased effective positive charge on the Lys side chain.

Molecular modeling and MD-based free energy calculation of LHPP-substrate complexes

The precise binding mode of the peptide substrate GGpKGG (**2a**, Fig. 6A) in complex with LHPP was unknown. Instead, a crystal structure of human LHPP has been available since 2010 in the protein database (RCSB PDB, ID: 2X4D), but has not been published anywhere else yet. This structure revealed the catalytic center of the LHPP comprising a phosphate group and a magnesium ion. In order to explore possible binding poses of **2a** within the catalytic center of LHPP, we performed a molecular docking study by defining Mg^{2+} in the catalytic center as the center of the docking pocket. Docking of **2a** into the pocket was carried out using the Glide module[38–40] implemented in the software Schrödinger.[41] Out of ten best docking poses with the highest scores, seven poses exhibited considerable overlap of the phosphate position of pLys with the one from the crystal structure. From these seven poses, we chose four poses (Fig. 6B & ESI, Section 4.6†), that showed significant variation in their binding conformations as the starting structures in the MD simulations. As no force field parameter for pLys can be found in the literature, we generated here the AMBER-based force field parameters for pLys using the previously proposed approach for

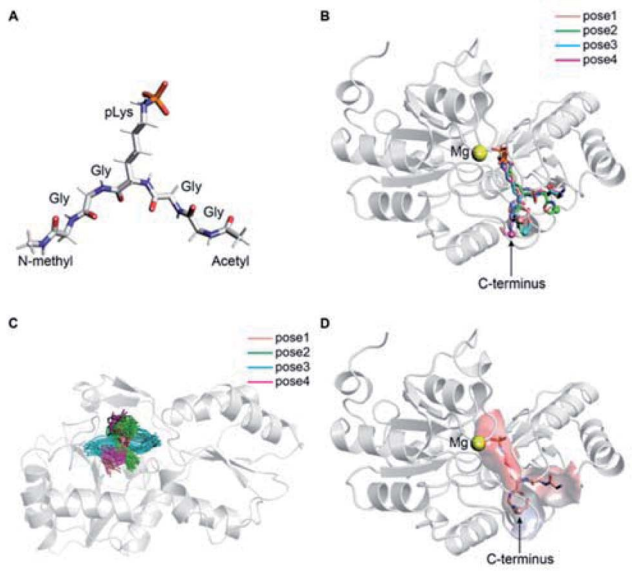

Fig. 6 (A) Molecular structure of model substrate **2a**. In the simulations *N*-methyl and acetyl were capped at C- and N-termini, respectively. (B) Overlaid docking poses of **2a** in the binding pocket of LHPP, showing pLys interacts with Mg^{2+}. Peptide **2a** in four different docking poses is shown as sticks with the C-terminal highlighted as sphere, and the LHPP as cartoon in grey. (C) Superposition of simulation snapshots of **2a** starting from 4 different docking poses. Peptides are shown as ribbon and LHPP as cartoon in grey. (D) Determined binding mode of **2a** in complex with LHPP (pose 1). Peptides are shown as ribbon with the C-terminal highlighted in sphere. LHPP is shown as cartoon and the electrostatic potential (red: negative, blue: positive) of the binding pocket has been mapped onto the molecular surface.

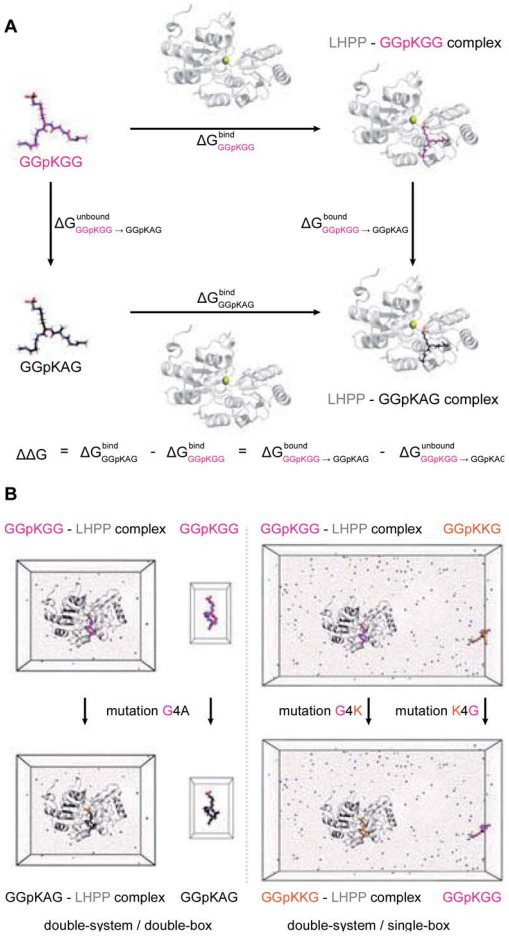

Fig. 7 (A) Thermodynamic cycle used in this study to calculate the free energy difference between the GGpKGG **2a** and other mutated peptides, *e.g.* GGpKAG **4a** or GGpKKG **4f**. (B) Double-system/double-box and double-system/single-box setups employed in the $\Delta\Delta G$ calculation of charge-conserving and charge-changing mutations, respectively.

parameterizing phosphorylated serine, threonine, tyrosine, and histidine.[42] Detailed procedure of the parameterization as well as newly introduced parameters of phosphorylated lysine are given in the ESI in Section 4.2, Tables S4 and S5.† During a 100 ns simulation of **2a** solvated in water, the energy values remained to be stable. Furthermore, no obvious molecular distortion was observed during the simulations, additionally verifying these new force field parameters of phosphorylated lysine to be suitable for the MD simulations.

In order to theoretically evaluate the free energy changes of different pLys-based pentapeptides, we employed alchemical free energy calculations for **3a**, **3f**, **3i**, **3j**, **4a**, **4f**, **4i** and **4j** using the non-modified peptide **2a** as the reference. **3a**/**4a** (Ala), **3f**/**4f** (Lys) and **3i**/**4i** (Arg) were selected in the simulations, as experimentally introducing these three amino acids in either C- or N-terminus showed large differences in their enzymatic activities (Fig. 4). As a comparison, we calculated free energy changes of **3j**/**4j** (Ser) relatively to **2a**, which revealed a remarkable decrease in the phosphoramidate hydrolase activity of LHPP when introducing the serine at both C- and N-termini.

The general idea of MD-based free energy calculation is illustrated in Fig. 7A. The method requires a combination of the equilibrium MD simulations to sample the conformational space of the non-modified and modified peptides, as well as fast non-equilibrium transitions from each other. In the equilibrium MD simulations of **2a** starting from four different docking poses, the binding conformations of the peptide remained relatively stable and did not interconvert to each other (Fig. 6C). In order to evaluate which docking pose represents the best binding conformation of the peptide, we performed the equilibrium simulations for **3a**, **3f**, **3i**, **3j**, **4a**, **4f**, **4i** and **4j**, respectively, starting from each four poses. The subsequent non-equilibrium alchemical transition simulations were carried out according to previously established protocol[43,44] using a combination of the GROMACS[45,46] and pmx[47,48] software packages. In the free energy calculations upon amino acid switching that cause a net charge change, we adopted the double-system/single-box setup,[49] while the charge-conserving simulations were performed using the double-system/double-box setup (Fig. 7B). Both Crooks Gaussian Intersection (CGI) and Bennet's Acceptance Ratio (BAR) estimators were employed in the analysis of free energy changes $\Delta\Delta G$.[44] Details of the simulations are given in the ESI in Section 4.4 & 4.5.†

Results summarized in Table S7† suggested that the predicted free energy changes upon amino acid changes in the peptide were considerably different for the simulations starting

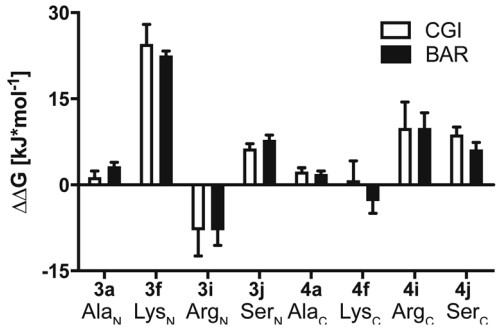

Fig. 8 Calculated ΔΔ*G* together with errors of mutated substrates relative to the WT model substrate **2a** estimated from the MD simulations starting from docking pose 1. Crooks Gaussian Intersection (CGI) and Bennet's Acceptance Ratio (BAR) estimators were employed for the analysis of ΔΔ*G*.

from different docking poses. Qualitatively, free energy changes derived from the simulations of the docking pose 1 revealed unambiguously the best agreement with the experimental data (Fig. 4 and 8). The large difference in free energy changes of **3f**/**4f** and **3i**/**4i** as well as a significant decrease of free energy in both **3j**/**4j** compared to the WT **2a** were all well reproduced in the simulations. Nevertheless, experimentally introducing the Ala at the N-terminal (**3a**) retained the hydrolysis yields, while the counter modification at the C-terminus (**4a**) diminished conversion. This result did not fit to the simulation data, as slight increases in relative binding free energy were predicted for both **3a**/**4a** compared to **2a**. We hypothesize that this was, because introducing small steric perturbation in amino acid sequence may require much longer simulation time than that was performed in the current study (a few hundred of nanoseconds) to capture the differences in binding.

In the best binding mode revealed by the alchemical free energy calculations (pose 1, Fig. 6D), the side chain of the pLys is nicely fitted in a small cavity that is negatively charged and completely buried from solvent, with the doubly charged magnesium ion compensating the negative charges both from the substrate and the protein environment. In contrast, electronic potential of the binding site for accommodating the substrate main chain was mostly negative. This was in good agreement with the enzymatic assay revealing peptides containing a negatively charged Asp residue (**3c**/**4c**) and showed considerably decreasing hydrolysis rate compared to the WT **2a** (Fig. 4). Nevertheless, we also observed significant difference in the electrostatic potential of the binding pocket for C- and N-termini regions (Fig. 6D), explaining the experimental finding that substrates with positively charged residues (**3f**/**4f** and **3i**/**4i**) exhibited very different enzymatic activity in their C- or N-terminus modifications (Fig. 4).

Conclusions

In conclusion, we present an integrated experimental and computational approach to evaluate the activity and binding affinity of an enzyme towards intrinsically labile substrates, for which no information about the substrate scope was available prior to our studies. Specifically, we elucidate the enzymatic reactivity of LHPP towards different *N*-and *O*-phosphorylated amino acids and peptides. Building upon reliable synthetic protocols to obtain a variety of phosphorylated substrates, we expand the previous reports by Hiraishi *et al.*[8,9] that LHPP acts as primarily as phosphoramidate hydrolase, for example on pLys or pHis. Furthermore, we studied in detail the sequence dependency in synthetic pLys substrates and observed a high sequence dependency rather than promiscuity on peptidic substrates. By applying molecular docking, we explored the possible binding poses of the non-modified peptide **2a** in the catalytic center of LHPP, which were further evaluated using MD-based alchemical free energy calculations. The latter calculations delivered precious insight into the sequence dependency of LHPP's enzymatic activity. The combination of biochemical assays and computational simulations suggested a defined binding mode of the labile substrates in complex with LHPP, which is difficult to establish using conventional approaches such as X-ray crystallography. Overall, in light of the recent emergence of labile phosphorylations, we show in a case study a novel binding event of LHPP specific for pLys substrates. Moreover, we strongly envision that this integrated approach can deliver valuable information about interactions of other enzymes with labile substrates.

Conflicts of interest

There are no conflicts to declare.

Acknowledgements

This research was supported by the DFG (SFB 765), the Evonik Stiftung (Doctoral fellowship to A. H.) and DFG under Germany's Excellence Strategy – EXC 2008 – 390540038 – UniSysCat. We thank Dr Jens von Kries for equipment support. The authors thank Prof. Maja Köhn for advice on the phosphatase assay. Furthermore, we also acknowledge the North-German Supercomputing Alliance (HLRN) for providing High Performance Computing (HPC) resources that have contributed to the research results reported in this paper.

Notes and references

1 J. A. Ubersax and J. E. Ferrell Jr, *Nat. Rev. Mol. Cell Biol.*, 2007, **8**, 530–541.
2 M. K. Tarrant and P. A. Cole, *Annu. Rev. Biochem.*, 2009, **78**, 797–825.
3 S. J. Humphrey, D. E. James and M. Mann, *Trends Endocrinol. Metab.*, 2015, **26**, 676–687.
4 G. Manning, G. D. Plowman, T. Hunter and S. Sudarsanam, *Trends Biochem. Sci.*, 2002, **27**, 514–520.
5 B. A. Haubrich and D. C. Swinney, *Curr. Drug Discovery Technol.*, 2016, **13**, 2–15.
6 M. J. Suskiewicz, B. Hajdusits, R. Beveridge, A. Heuck, L. D. Vu, R. Kurzbauer, K. Hauer, V. Thoeny, K. Rumpel, K. Mechtler, A. Meinhart and T. Clausen, *Nat. Chem. Biol.*, 2019, **15**, 510–518.

7 S. Fahs, P. Lujan and M. Köhn, *ACS Chem. Biol.*, 2016, **11**, 2944–2961.
8 H. Hiraishi, T. Ohmagari, Y. Otsuka, F. Yokoi and A. Kumon, *Arch. Biochem. Biophys.*, 1997, **341**, 153–159.
9 H. Hiraishi, F. Yokoi and A. Kumon, *Arch. Biochem. Biophys.*, 1998, **349**, 381–387.
10 F. Yokoi, H. Hiraishi and K. Izuhara, *J. Biochem.*, 2003, **133**, 607–614.
11 E. Koike, S. Toda, F. Yokoi, K. Izuhara, N. Koike, K. Itoh, K. Miyazaki and H. Sugihara, *Biochem. Biophys. Res. Commun.*, 2006, **341**, 691–696.
12 J. Zheng, X. Dai, H. Chen, C. Fang, J. Chen and L. Sun, *Biochem. Biophys. Res. Commun.*, 2018, **503**, 1108–1114.
13 S. K. Hindupur, M. Colombi, S. R. Fuhs, M. S. Matter, Y. Guri, K. Adam, M. Cornu, S. Piscuoglio, C. K. Y. Ng, C. Betz, D. Liko, L. Quagliata, S. Moes, P. Jenoe, L. M. Terracciano, M. H. Heim, T. Hunter and M. N. Hall, *Nature*, 2018, **555**, 678.
14 Y. Li, X. Zhang, X. Zhou and X. Zhang, *Biosci. Rep.*, 2019, **39**(7), BSR20182270.
15 A. M. Burroughs, K. N. Allen, D. Dunaway-Mariano and L. Aravind, *J. Mol. Biol.*, 2006, **361**, 1003–1034.
16 H. Jung, S. H. Shin and J.-M. Kee, *ChemBioChem*, 2019, **20**, 623–633.
17 A. Gohla, *Biochim. Biophys. Acta, Mol. Cell Res.*, 2019, **1866**, 153–166.
18 Y. Choi, S. H. Shin, H. Jung, O. Kwon, J. K. Seo and J.-M. Kee, *ACS Sens.*, 2019, **4**, 1055–1062.
19 D. L. Smith, B. B. Bruegger, R. M. Halpern and R. A. Smith, *Nature*, 1973, **246**, 103–104.
20 D. L. Smith, C.-C. Chen, B. B. Bruegger, S. L. Holtz, R. M. Halpern and R. A. Smith, *Biochemistry*, 1974, **13**, 3780–3785.
21 C. C. Chen, B. B. Bruegger, C. W. Kern, Y. C. Lin, R. M. Halpern and R. A. Smith, *Biochemistry*, 1977, **16**, 4852–4855.
22 C.-C. Chen, D. L. Smith, B. B. Bruegger, R. M. Halpern and R. A. Smith, *Biochemistry*, 1974, **13**, 3785–3789.
23 J. Bertran-Vicente, R. A. Serwa, M. Schümann, P. Schmieder, E. Krause and C. P. R. Hackenberger, *J. Am. Chem. Soc.*, 2014, **136**, 13622–13628.
24 K. Adam, S. Fuhs, J. Meisenhelder, A. Aslanian, J. Diedrich, J. Moresco, J. La Clair, J. R. Yates and T. Hunter, *bioRxiv*, 2019, 691352, DOI: 10.1101/691352.
25 G. Hardman, S. Perkins, P. J. Brownridge, C. J. Clarke, D. P. Byrne, A. E. Campbell, A. Kalyuzhnyy, A. Myall, P. A. Eyers, A. R. Jones and C. E. Eyers, *EMBO J.*, 2019, **38**, e100847.
26 J. Bertran-Vicente, M. Penkert, O. Nieto-Garcia, J.-M. Jeckelmann, P. Schmieder, E. Krause and C. P. R. Hackenberger, *Nat. Commun.*, 2016, **7**, 12703.
27 J. Bertran-Vicente, M. Schümann, C. P. R. Hackenberger and E. Krause, *Anal. Chem.*, 2015, **87**, 6990–6994.
28 J. Bertran-Vicente, M. Schümann, P. Schmieder, E. Krause and C. P. R. Hackenberger, *Org. Biomol. Chem.*, 2015, **13**, 6839–6843.
29 M. Penkert, A. Hauser, R. Harmel, D. Fiedler, C. P. R. Hackenberger and E. Krause, *J. Am. Soc. Mass Spectrom.*, 2019, **30**, 1578–1585.
30 J. D. Chodera, D. L. Mobley, M. R. Shirts, R. W. Dixon, K. Branson and V. S. Pande, *Curr. Opin. Struct. Biol.*, 2011, **21**, 150–160.
31 B. J. Williams-Noonan, E. Yuriev and D. K. Chalmers, *J. Med. Chem.*, 2018, **61**, 638–649.
32 S. Michielssens, J. H. Peters, D. Ban, S. Pratihar, D. Seeliger, M. Sharma, K. Giller, T. M. Sabo, S. Becker, D. Lee, C. Griesinger and B. L. de Groot, *Angew. Chem., Int. Ed.*, 2014, **53**, 10367–10371.
33 K. Hauser, C. Negron, S. K. Albanese, S. Ray, T. Steinbrecher, R. Abel, J. D. Chodera and L. Wang, *Commun. Biol.*, 2018, **1**, 70.
34 M. R. Webb, *Proc. Natl. Acad. Sci. U. S. A.*, 1992, **89**, 4884–4887.
35 H. R. Matthews, *Pharmacol. Ther.*, 1995, **67**, 323–350.
36 Y.-F. Wei and H. R. Matthews, in *Methods Enzymol.*, ed. B. M. S. Tony Hunter, Academic Press, 1991, vol. 200, pp. 388–414.
37 F. T. Hofmann, C. Lindemann, H. Salia, P. Adamitzki, J. Karanicolas and F. P. Seebeck, *Chem. Commun.*, 2011, **47**, 10335–10337.
38 R. A. Friesner, J. L. Banks, R. B. Murphy, T. A. Halgren, J. J. Klicic, D. T. Mainz, M. P. Repasky, E. H. Knoll, M. Shelley, J. K. Perry, D. E. Shaw, P. Francis and P. S. Shenkin, *J. Med. Chem.*, 2004, **47**, 1739–1749.
39 T. A. Halgren, R. B. Murphy, R. A. Friesner, H. S. Beard, L. L. Frye, W. T. Pollard and J. L. Banks, *J. Med. Chem.*, 2004, **47**, 1750–1759.
40 R. A. Friesner, R. B. Murphy, M. P. Repasky, L. L. Frye, J. R. Greenwood, T. A. Halgren, P. C. Sanschagrin and D. T. Mainz, *J. Med. Chem.*, 2006, **49**, 6177–6196.
41 L. Schrödinger, in *Schrödinger Release 2018-1*, New York, 2018.
42 N. Homeyer, A. H. C. Horn, H. Lanig and H. Sticht, *J. Mol. Model.*, 2006, **12**, 281–289.
43 M. Aldeghi, V. Gapsys and B. L. de Groot, *ACS Cent. Sci.*, 2018, **4**, 1708–1718.
44 M. Aldeghi, B. L. de Groot and V. Gapsys, in *Computational Methods in Protein Evolution*, ed. T. Sikosek, Springer New York, New York, NY, 2019, pp. 19–47, DOI: 10.1007/978-1-4939-8736-8_2.
45 B. Hess, C. Kutzner, D. van der Spoel and E. Lindahl, *J. Chem. Theory Comput.*, 2008, **4**, 435–447.
46 M. J. Abraham, T. Murtola, R. Schulz, S. Páll, J. C. Smith, B. Hess and E. Lindahl, *SoftwareX*, 2015, **1–2**, 19–25.
47 D. Seeliger and B. L. de Groot, *Biophys. J.*, 2010, **98**, 2309–2316.
48 V. Gapsys, S. Michielssens, D. Seeliger and B. L. de Groot, *J. Comput. Chem.*, 2015, **36**, 348–354.
49 V. Gapsys, S. Michielssens, J. H. Peters, B. L. de Groot and H. Leonov, Calculation of Binding Free Energies, in: *Molecular Modeling of Proteins, Methods in Molecular Biology (Methods and Protocols)*, ed. A. Kukol, Humana Press, New York, NY, 2015, vol. 1215, DOI: 10.1007/978-1-4939-1465-4_9.